Investigation of the nanostructural background of functionality in case of biogenic and biocompatible mineral apatite (2017 December-2022 November)

Principal investigator: Viktória Kovács Kis

Participants: Zsolt Czigány, Zsolt Kovács, Attila Sulyok, István Dódony, György Radnóczi, Klára Hajagos-Nagy (2019-2021 maternity leave), Noémi Katinka Rózsa (from 2020), Katalin Balázsi, Zsolt Fogarassy, Zsolt Dallos (as PhD student in 2018, supervisor István Dódony).

Fanni Misják left to Ulm University (Germany) in 2019 and left Centre for Energy Research in 2020.

Undergaduate students involved in the project: Máté Hegedűs (Eötvös University, supervisor: Viktória Kovács Kis, Zsolt Kovács), Dániel Takács (Óduda University, Technical University of Budapest, supervisor: Attila Sulyok), András Szabó (Eötvös University, supervisor: Viktória Kovács Kis)

Project summary (based on the submitted proposal)

The aim of the project was to understand the crystal chemical background of the high capacity for adaptation to the different functions of biogenic apatites, on the nanometre scale and establish its application in biomimetic synthesis of nanocrystalline apatite. Biogenic apatites, like bone and enamel apatite, have tissue specific functions, which require tailored chemical and physical properties like crystallinity, hardness, solubility, stability. The formation of biogenic apatites is controlled biochemically at the cellular level. Understanding the nanostructure and hierarchical organization of biogenic apatites allows a deeper insight into their growth mechanisms and paves the way for an improved fine-tuning of biomaterial properties.

Methodology of electron diffraction

According to the original workplan, standardization of selected area electron diffraction (SAED) measurements for quantitative electron diffraction and validation of full profile analysis methods (electron Pair Distribution Function (ePDF), Rietveld) was an essential part of the investigation. ePDF is well suited for the quantitative structure analysis of amorphous and poorly crystalline materials, while electron diffraction based Rietveld analysis is applied for nanocrystalline materials. The main advantage of both methods, which were used during the analysis of biogenic apatites and phosphate biomaterials, is that they provide statistically meaningful structural information on nanostructured materials. During the project, both ePDF analysis and electron diffraction based Rietveld analysis have been optimized for the analysis of nanocrystalline apatites. ePDF optimization is detailed in relation with the study of bioactive glasses and in vitro apatite formation and Rietveld optimization is detailed in relation with dental enamel investigation.

Results 1: Formation and nanostructure of biomaterial hydroxylapatite

According to the original workplan, quantitative SAED was planned on biosynthetic hydroxylapatite biomaterial (BHB) synthesized at the Thin Film Physics Laboratory of the Centre for Energy Research (see e.g. Balázsi et al., J. Eur. Ceramic Society 27. (2007) 1601–1606) with the aim to discuss it in relation with the nanostructure of biogenic apatites. Detailed transmission electron microscopy (TEM) analysis of this material revealed that it contains three different Ca-phosphate phases. In addition, the size distribution of the crystallites exhibited a wide range (from the nanometre up to micrometre scale). Based on these observations, we ruled out the further analysis of BHB. Instead, in collaboration with Dr. Margit Fábián (Centre for Energy Research) a compositional series of phosphate doped silicate glass (SiO_2(45)CaO(25)Na_2O(30 - x)P_2O_5(x), where x = 0,1,3,5) was used as starting material for the in vitro

crystallization of hydroxylapatite. ePDF and neutron diffraction (ND) measurements were carried out in parallel.

Results 1.1: ePDF analysis of phosphate containing bioactive glasses [Kis et al. 2018 Ulm, invited talk, Fabian et al. 2020, Journal of Materials Science]

ePDF was used to characterize local structural fluctuation in bulk glasses and to follow the in vitro formation of hydroxylapatite containing bioactive layer. The data collection procedure for ePDF (electron Pair Distribution Function) analysis, and the effect of sample thickness and cutoff distance on the results of ePDF analysis was detailed in [Kis et al, 2018, Ulm, invited talk]. We demonstrate that the position of the peaks with real structural information remains unchanged independent of the cutoff distance, while peaks originating from the termination of the scattering angle range, migrate with cutoff position. Similarly, fitting parameters of the linear start of g(r), i.e. atomic density and minimum interatomic distance, are strongly dependent on cutoff position (Figure 1).

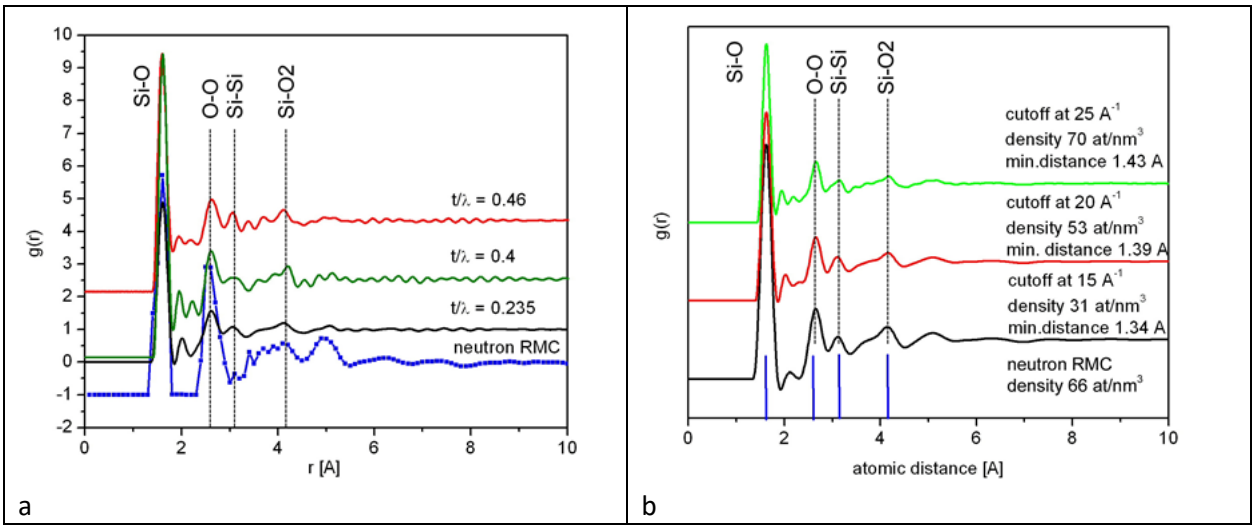

Figure 1 (a) ePDFs of amorphous silica with different thicknesses compared to neutron diffraction based PDF. Measurement at 300keV, measured area 25 nm in diameter, cutoff at 25 $Å^{-1}$. Thickness of the sample (t) normalized with the λ mean free path, i.e. (t/λ) ratios were measured using EELS. (b) ePDFs of a-SiO_X thin film applying different cutoff positions to the same measurement (200keV). Peak positions from Reverse Monte Carlo simulations based on neutron diffraction data are marked by blue sticks. [Fabian et al. 2020]

A detailed analysis of scattering contributions has been carried out on the studied compositions, which revealed that cation-O contributions in the electron diffraction (ED) measurement are quite similar to those in neutron diffraction (ND) measurement implying that the reliability of these correlations and the derived first-neighbour distances will be similar as well. As ND has well established quantitative evaluation methods (Reverse Monte Carlo applied in [Fabian et al 2020]), our structure factor analysis supports that ED measurements on small volumes of Ca-P-(Si-Na)-O containing materials (e.g. bioactive silicate glass, bioapatite, and other, nanocrystalline phosphates) provide reliable structural data. The structure factor analysis also demonstrates that in the case of electron scattering cation-oxygen contributions comprise only 50% of the overall scattering (for neutron scattering the same ratio is 90%). This implies a significant cation–cation contribution in case of ED, which carries structural information on how the silicate tetrahedra are connected to each other, i.e. the medium-range order can be quantified. Making use of the locality of electron scattering, position dependent structural fluctuations were revealed in phosphate

doped bioactive glass (Figure 2), and related to the formation of phosphate rich clusters. This finding was in agreement with the thermal behaviour of the glasses and confirmed by high resolution transmission electron microscopy (HRTEM) and was published in an integrated bulk-to-nanoscale study [Fabian et al. 2020].

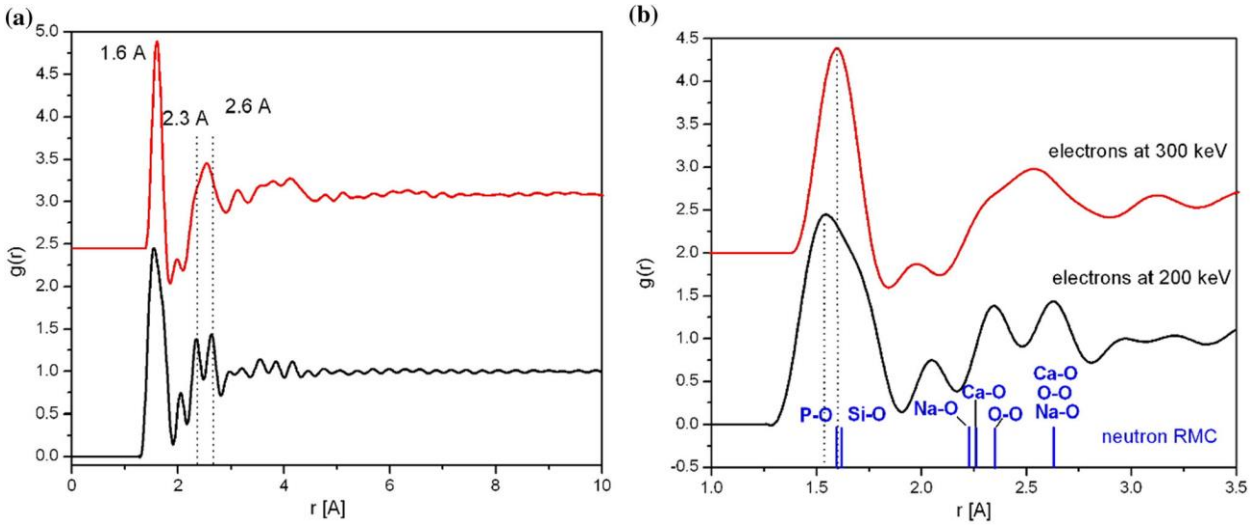

Figure 2: (a) Total pair distribution functions from electron diffraction measurements, (b) low r range of the total pair distribution functions from electron diffraction measurements with the indicated first-neighbour distances determined by neutron-based RMC simulation. [Fabian et al. 2020]

Results 1.2: In vitro formation of hydroxylapatite: nanostructural and nanomechanical studies [Kis et al. 2018 MMT talk, Kovacs et al. 2022, Journal of Non-Crystalline Solids]

In vitro formation of nanocrystalline hydroxylapatite was followed by incubating the bulk glasses in simulated body fluid (SBF) for different timespans at 37 °C and p(CO_2) = 0.05 atm (5%). According to ePDF analysis, phase separation initiates in the amorphous state (Figure 3) and composition fields of the two amorphous structures could be identified (Figure 4). [Kis et al. 2018 – MMT talk] To complete the average nanostructure information, high resolution transmission electron microscopy (HRTEM) was performed at locations with different P:Si ratio (Figure 5).

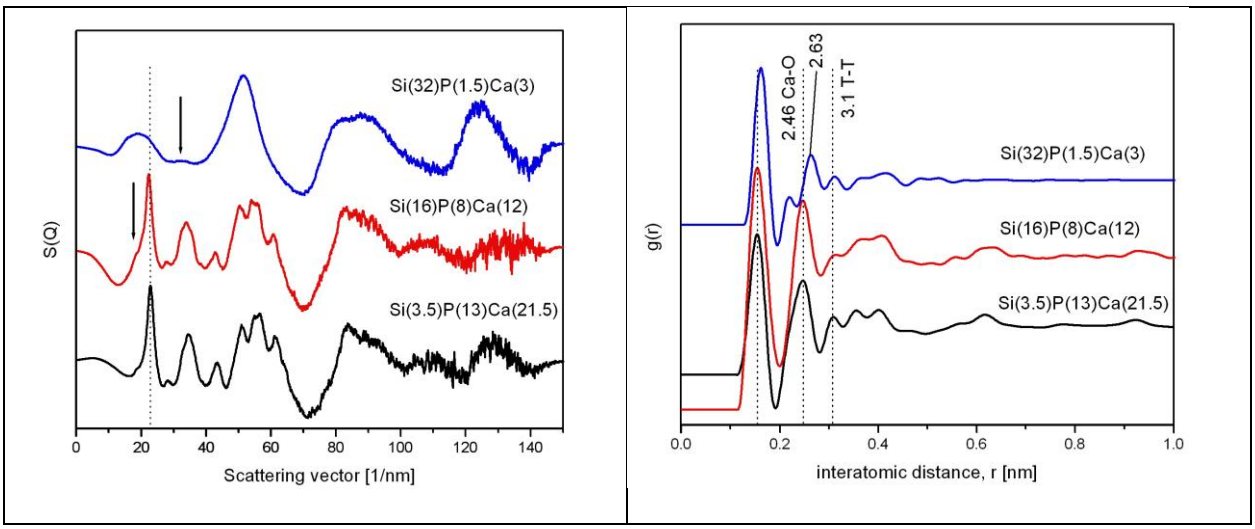

Figure 3 (a) Reduced interference functions and (b) corresponding pair distribution functions of bioactive layer at three different compositions. Fast Fourier transforms (FFT) of HRTEM images clearly indicate that with increasing phosphorus content, the crystallinity increases as well. Full length paper is in preparation based on the results presented in [Kis et al. 2018 MMT talk].

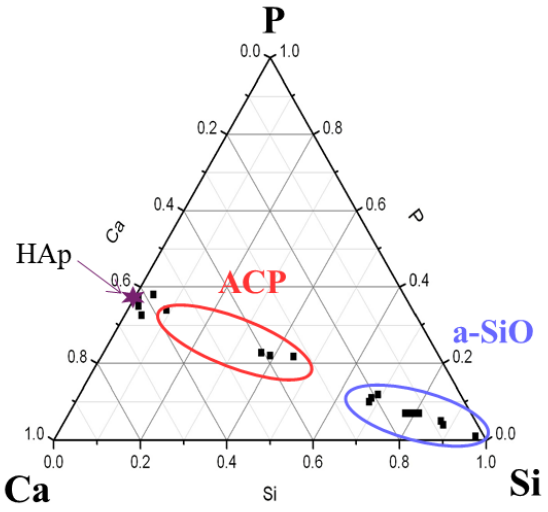

Figure 4: Ternary diagram used to plot the Si:P:Ca ratios measured at different locations in the bioactive layer. Each point represents a TEM-EDS measurement with an ePDF analysis. Based on ePDF analysis, amorphous SiO_2 structure is stable if P:Si < 0.35. If 0.5 <P:Si < 0.95, amorphous Ca-phosphate structure forms. If P:Si > 0.95, nanocrystalline hydroxylapatite forms. [Kis et al. 2018 MMT talk]

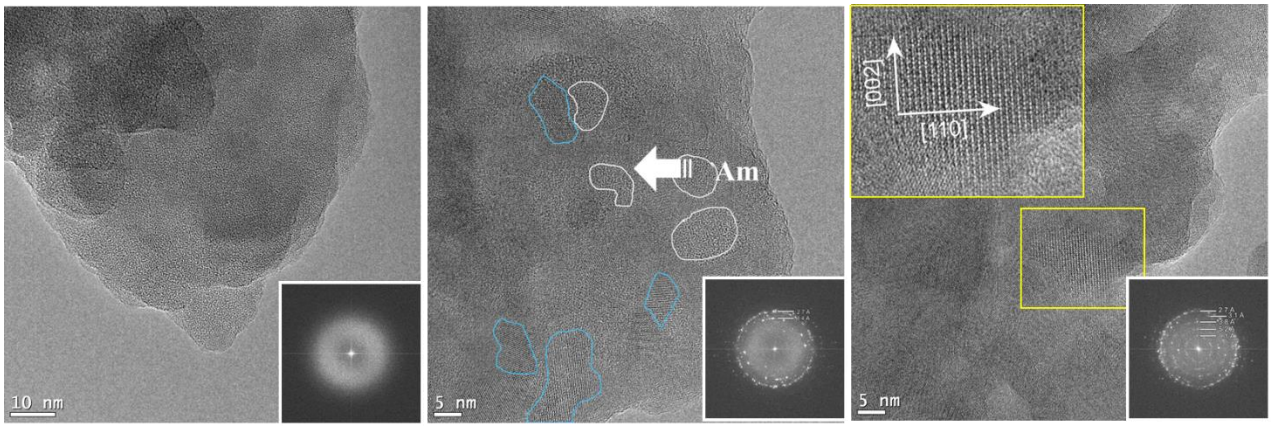

Figure 5: HRTEM images of the bioactive layer. As indicated by the FFTs in the corner of the images, crystallinity increases from the left to the right. On the middle image, few nanometre sized amorphous (white) and nanocrystalline (blue) areas can be distinguished in close vicinity. On the right, nanocrystalline hydroxylapatite domain is indexed. [Kis et al. 2018 MMT talk]

The initial stage of the *in vitro* bioactive layer formation on the surface of the bioactive glasses was investigated in detail, by means of focussed ion beam milling (Figure 6) assisted scanning electron microscopy and nanoindentation [Kovacs et al. 2022, Journal of Non-Crystalline Solids].

Bioactive layer formation initiates by formation of a transient amorphous Ca-phosphate phase and followed by crystallization of nanocrystalline hydroxylapatite, which, under *in vivo* conditions, triggers bonding to bone tissue. We found that the hardness of the untreated samples increases with PO_4 content up to 3 mol% phosphate concentration and no further increase was observed for the 5 mol% PO_4 sample. Nanoindentation tests after 30 min SBF treatment indicate a severe decrease of the hardness for all samples with respect to the untreated glasses. The change of mechanical properties was explained in terms of network structure parameters of the glasses. Change of the Young's modulus (E) and the Vickers

hardness (HV) via the HV/E ratio, as function of phosphate content before and after SBF treatment was discussed (Figure 7), and the characteristics related to chemical bonding and plastic deformation were separated.

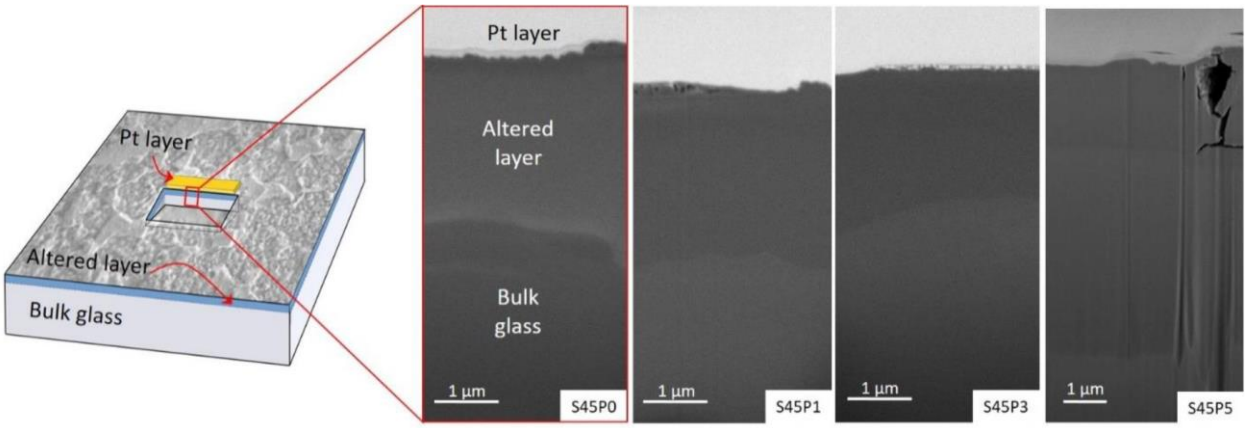

Figure 6: Back-scattered electron SEM images of the cross-sections of SBF treated surfaces of the S45P0, S45P1, S45P3, and S45P5 bioactive glass samples from [Kovacs et al. 2022, Journal of Non-Crystalline Solids]

Variation of the P content in the untreated glasses resulted in minor change in the Young's modulus. At the same time, severe P content dependent increase in the HV/E ratio was observed up to about 2-3 mol% concentration (Figure 7d). At this composition, the silicate network connectivity $N(BO)_{Si}$ is approximately 2, which indicates that continuous -Si-O-Si- chains become interconnected in the glass (Figure 7e). In parallel, the theoretical yield strength (at about HV/E≈0.06 - 0.09), which is a general strength limit for solid materials, is reached at the same composition.

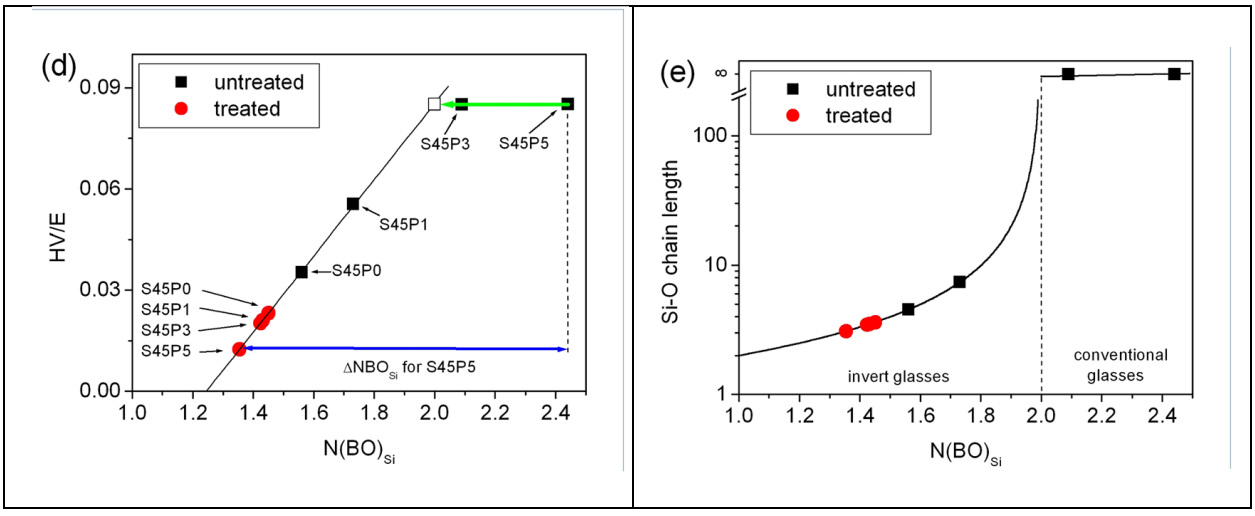

Figure 7: (d) Scaling between HV/E and N(BO)Si. (e) Average Si-O chain length calculated from N(BO)Si for the studied compositions from [Kovacs et al. 2022, Journal of Non-Crystalline Solids]

This coincidence indicates two conclusions. (1) Besides the amount of soft structural defects (Si-O-Ca/Na NBO sites), the formation of a strong continuous -Si-O-Si- network has a key role in the plastic behaviour. (2) The HV/E ratio is a good parameter for quantitative characterization of the network structure through

the correlation with -Si-O-Si- chains length in the $1<N(BO)_{Si}<2$ range (up to the theoretical yield strength). These considerations were applied for a quantitative estimation of the structural evolution during SBF treatment in the very early stage of the reaction. Thus, according to our results, nanoindentation allows assessment of bioactivity of any newly formulated glass composition without the need of long lasting soaking experiments.

Results 2: Crystal chemistry of bone apatite [Dallos et al. 2018 Sydney IMC poster, Kis et al. 2019 Materials Science and Engineering C paper, Dallos et al. 2020 Cryst. Eng. Comm. paper]

This part of the project was investigated with the active participation of Dr. Zsolt Dallos, former PhD student of Prof. István Dódony at Eötvös University (PhD defence in 2020).

HRTEM investigation proved to be a more effective tool providing informative analysis on the nanostructure of bone apatite than electron diffraction methods. Using an Upper Cretaceous turtle plate sample we performed an atomic level investigation of individual bone apatite nanocrystals. Crystallographic image processing of the obtained HRTEM images from different projections indicated symmetry reduction with respect to $P6_3/m$ stoichiometric apatite and the presence of threefold symmetry along the c axis (Figure 8). Based on HRTEM observations and the measured Ca/P=2 ratio we proposed a structural model with phosphate-to-carbonate substitution and O vacancies localized along c axis, which explained the observed loss of 6_3 screw axis parallel with the c axis, and the 1⁄4 c shift of the mirror plane.

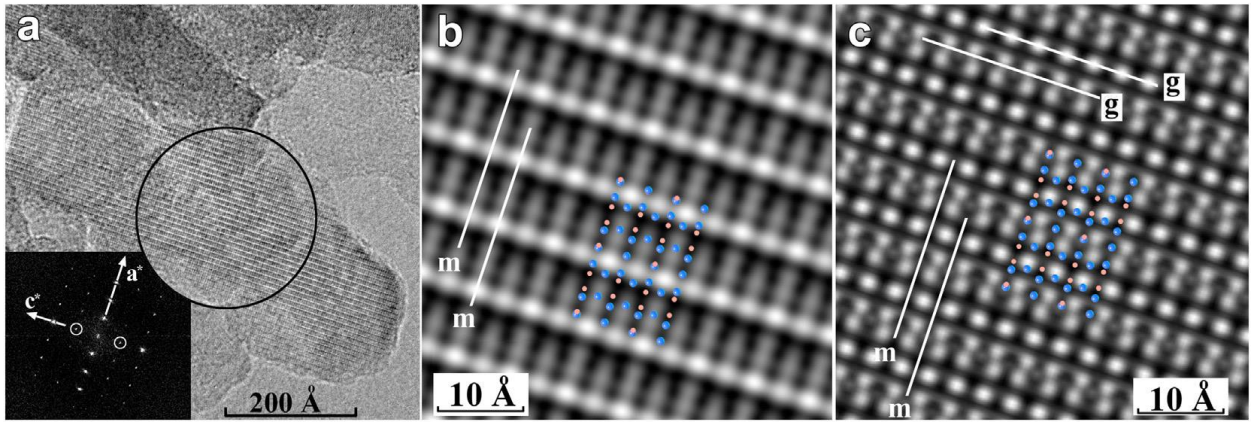

Figure 8: (a) [100] HRTEM image of bone apatite nanocrystal with its Fourier transform inserted in the lower left corner. Fourier components forbidden by $P6_3/m$ space group symmetry are encircled. (b) Enlarged symmetry imposed image, mirror planes (m) are marked. The inset is the structure model of $P6_3/m$ apatite for 2×2 unit cells. (c) Calculated [100] HRTEM image of $P6_3/m$ F-apatite with 2 Å resolution. The 2D symmetry elements, mirror plane (m) and glide plane (g), are marked. The inset is the structure model of $P6_3/m$ apatite for 2×2 unit cells. Calcium (orange) and phosphorus (blue) atoms are shown, other atoms are omitted for clarity. [Kis et al. 2019, Materials Science and Engineering C]

Besides symmetry reduction, we give evidence for polarity along [010] direction of bone apatite which implies chemically distinct (0*k*0) surfaces and propose that the relative orientation of (0*k*0) facets with respect to the collagen fibre has prominent role in resorption processes and also in the adhesion of apatite nanocrystals to collagen fibers. Our results highlight the function of surface chemistry and indicate that biochemically controlled crystallization produces highly functionalized nanocrystals. Actually, we are performing measurements for similar analysis on apatite nanocrystals freshly extracted from ewe bone by immersion in NaClO obtained via an informal collaboration with Prof. Henry Schwarcz (McMaster University, Canada).

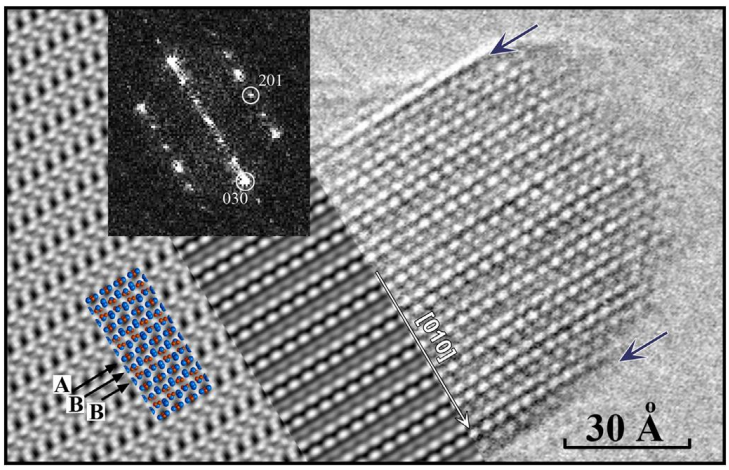

Figure 9. [10−2] HRTEM image of a bone apatite nanocrystal. The right part is the original image, the middle part was filtered using Fourier maxima and the left part is the simulated HRTEM. The inset is the Fourier transform. The structure model shows the position of the calcium (blue) and phosphorus (orange) atoms, other atoms are omitted for clarity. Pair of arrows in the original image indicate positive and negative (010) terminations. [Kis et al. 2019, Materials Science and Engineering C]

For a better understanding of the crystal chemistry of bone apatite, solubility experiments and heat treatment has been carried out on bovine bone apatite. We studied leaching of powdered bovine tibia in carbonate saturated water (using $NaHCO_3$) as a function of concentrations and treating periods [Dallos et al. 2020 Cryst. Eng. Comm.]. According to our results, the $[CO_3]^{2-}$ substitution in apatite is limited, does not exceed one $[CO_3]^{2-}$ per unit cell, which is in agreement with our proposed structure model in [Kis et al. 2019 MSEC]. When the amount of $[CO_3]^{2-}$ becomes higher, the apatite structure destabilizes and dissolves. Based on HRTEM images, residual nanocrystalline apatite and unstable Ca-carbonate were also recognized allowing the reconstruction of intermediate stages of leaching process (Figure 10). Finally, we conclude that the carbonate-to-phosphate transformation is a reversible process which has significant implications for environmental geology, fossilization, medical, applied material engineering and for the investigation of pathological lesions as well.

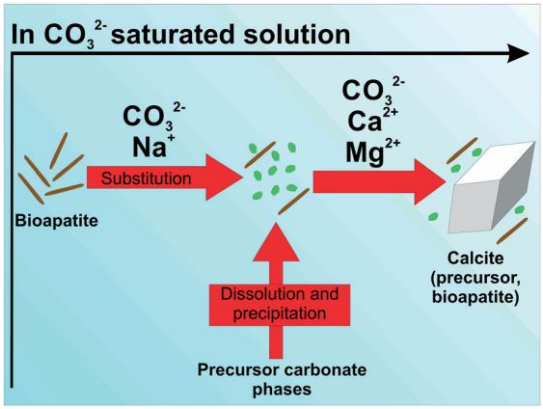

Figure 10: Schematic of the dissolution–precipitation process. [Dallos et al. 2020 Cryst. Eng. Comm.]

Heat treatment of bovine bone sample was made in the temperature range 25-1100°C and structural alterations were studied by (HR)TEM. According to our observations, recrystallization begins over 400 °C, simultaneously with the organic component breakdown. Above this temperature, transformation of the nano-polycrystalline aggregates to larger, $P6_3/m$ apatite single crystals is dominant. Crystallite size kept increasing up to 700°C, which is interpreted as recrystallization and sintering-like adherence of nanocrystals [Dallos et al. 2018. Sydney IMC poster]. These results explain the inhomogeneous crystallite size of biosynthetic hydroxylapatite biomaterial (BHB), which has been prepared above 900°C, and indicate the need of fine-tuning of the post sintering mechanical milling procedure to obtain nanocrystalline material.

Results 3: Correlation of crystal chemistry and mechanical properties of dental enamel

After thorough overview of the relevant literature, we decided to focus on primary teeth mainly for the following reasons. (1) The mechanical properties of primary tooth enamel is much less known than that of permanent tooth enamel, and (2) in primary tooth enamel the outer aprismatic layer is preserved with higher probability, which may exhibit distinct performance with respect to the better known prismatic layer of permanent tooth. The research procedure applied to dental enamel was approved by the Ethics Committee of the Semmelweis University, Budapest (approval no. 84/2020). This part of the project was investigated with the active participation of Mr. Máté Hegedűs (Eötvös University BSc, MSc thesis, actually PhD student) and Mr. Dániel Takács (Óbuda University BSc thesis, actually Technical University of Budapest, MSc student).

Results 3.1 Gradient anisotropy in dental enamel [Hegedűs MSc thesis 2021, Hegedűs et al. submitted, Hegedűs et al. in prep. Hegedűs et al. 2022 MMT talk]

Mechanical properties of sound primary dental enamel were studied as function of depth from surface using nanoindentation mapping, and correlated with chemical composition, nanocrystal and prism orientation. Prism orientation distribution was quantified as function of aspect ratio and inclination angle through the whole cross section (Figure 11). Actually we are preparing a manuscript focusing on the methodology of prism orientation mapping [Hegedűs et al. in prep]. In parallel, the application of Raman mapping for the analysis of crystal orientation distribution is also in progress (Hegedűs et al. 2022 MMT talk).

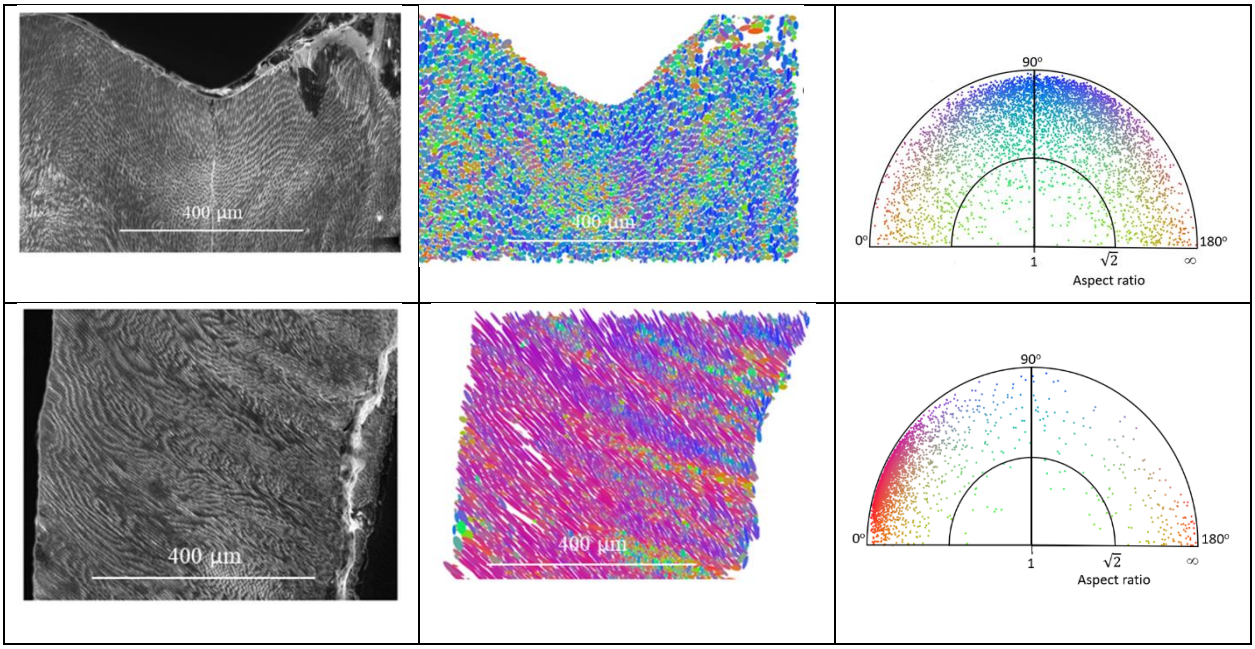

Figure 11 Secondary electron SEM images of etched surfaces (left) and corresponding enamel prism orientation maps obtained by ellipse fitting method (middle). The colours represent aspect ratio and azimuthal inclination of prisms in the image plane. On the right, two dimensional probability distribution diagrams of prism orientations are seen. [Hegedűs et al. submitted]

When analysing nanoindentation data, we followed the same procedure as in case of bioactive glasses and normalized the HV with the modulus E. We found that based on HV and E, mechanical properties could not be directly linked to crystal chemistry, while the spatial variation of HV/E exhibited good correlation with changes of average crystal chemistry, namely Ca/P ratio and trace element concentration.

Based on nanoindentation measurements performed on hydroxyapatite single crystal, and subsequent theoretical considerations we found that modulus normalized nanohardness is independent of crystal orientation. Thus, the spatial variation of HV/E measured in enamel can be related either to structural defects or changing volume fraction organic material reported in the literature.

Quantitative estimation of the relative contribution of prism orientation and crystal chemistry to the mechanical response of enamel was provided, and orientation dependent and composition dependent components of hardness and elastic modulus were plotted separately as function of depth from the surface (Figure 12).

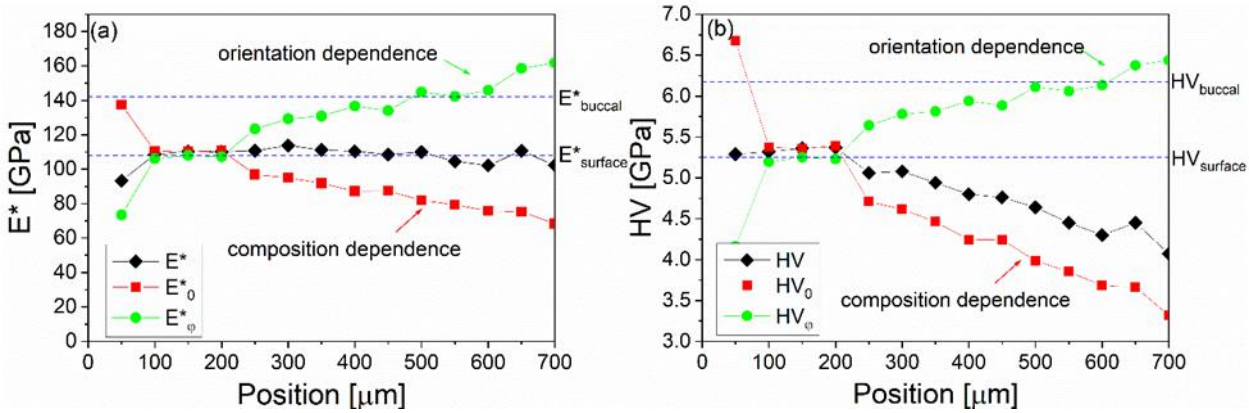

Figure 12: Position dependence of mechanical properties and microstructure of enamel prisms in the distal-mesial cross section. [Hegedűs et al. submitted]

Composition dependent parts of the hardness and elastic modulus are monotonously decreasing from the outer surface towards the dentin-enamel junction (DEJ indicating gradual change of average chemistry, which is in agreement with literature data on organic material content, Ca/P ratio and trace element concentrations. Orientation dependent parts of hardness and elastic modulus are monotonously increasing from the outer surface towards the DEJ, indicating the change in prism arrangement due to the Hunter-Schreger bands. Average prism orientation as function of distance from DEJ calculated using experimental hardness and elastic modulus data agrees well with that obtained from prism inclination measured directly on orientation maps. Separation of prism orientation and chemistry dependent parts of hardness and elastic modulus highlights the elastic anisotropy of the enamel. In addition, it demonstrates that the modulus is nearly constant for the whole enamel volume if measured in cross section, while exhibits negative gradient towards the DEJ if viewed down the buccal direction.

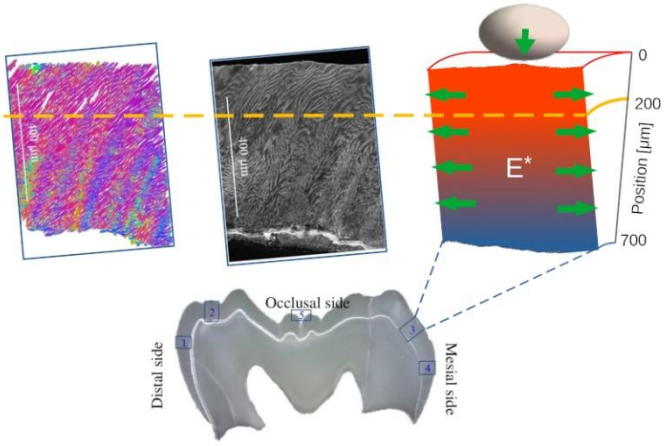

Figure 13: Prism orientation change involves average orientation change of nanocrystals. Gradual change in prism orientation implies gradually changing mechanical anisotropy. The hierarchical structure smoothens and tunes mechanical anisotropy of the single crystal and ensures resistance of dental enamel to axial loads and opening stresses at the same time. We think that this is the clue to the unique mechanical performance of dental enamel. [Hegedűs et al. submitted]

Such variation of modulus guarantees the unique combination of high surface strength and good crack resistance for dental enamel. These findings reveal the synergistic effect of morphology and crystal chemistry, creating and fine tuning the mechanically graded structure of dental enamel (Figure 13).

Results 3.2 Mg exchange [Hegedűs BSc thesis 2019, Kis et al. 2021 Acta Biomater, Kis et al. 2022 ELMINA poster]

Apatite nanocrystals in biological hard tissues crystallize in a certain range of physiological parameters, which allows individual variation of the performance. We studied by nanoindentation mapping a primary dental enamel sample in cross section, which, according to routine visual observation proved to be sound and does not exhibited any deviation from the average. A pronounced hardness increase was measured in the outer 200 µm zone, which was accompanied by an unusual enrichment of Mg in the same zone. The highest Mg content (1 at%) was measured at about 150 µm from the outer surface (Figure 14).

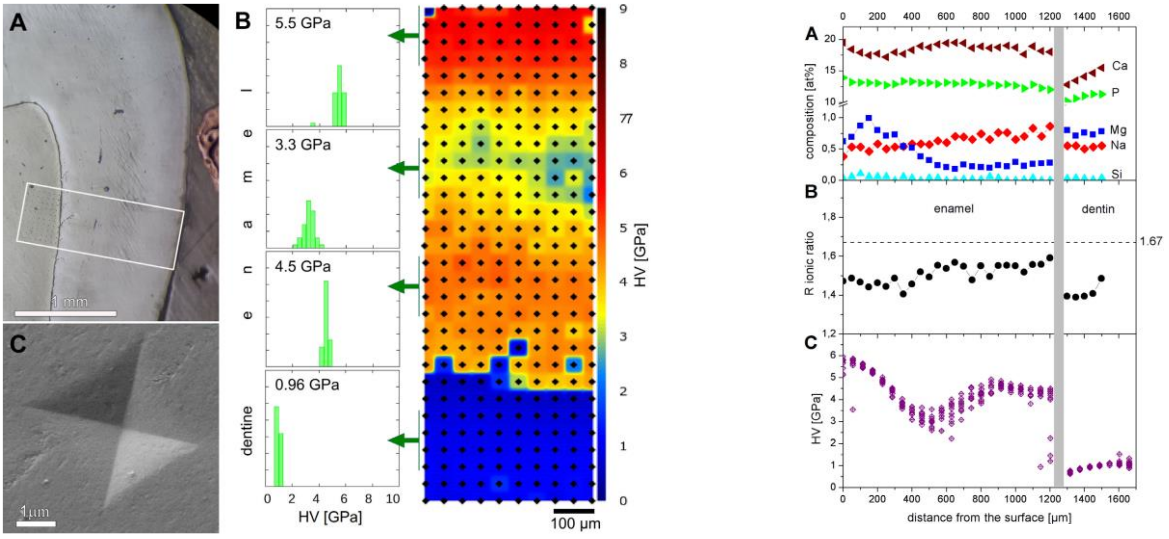

Figure 14: (left) (A) The area subjected to the nanoindentation tests is marked with white box on the optical micrograph. (B) Hardness map of the marked area with color coded Vickers hardness values. The insets show the hardness frequency distributions and the average hardness values of 4 ×10 tests at

different selected depths in the enamel and in the dentin. (C) SEM image of a Vickers imprint in the enamel, showing its typical shape and size. (right) (A) Compositional data obtained from SEM-EDS line profile analysis from the enamel surface towards the enamel-dentin junction and dentin. (B) R ionic ratio calculated from the SEM-EDS results and (C) hardness values obtained from nanoindentation tests near the same cross-sectional area shown on the left. [Kis et al. 2021 Acta Biomater]

To investigate if the elevated Mg content contributes to the increased hardness, we followed the pilot study of Abdallah et al. (Acta Biomater. 37 (2016) 174–183) and performed Mg exchange experiments on the outer surface of sound primary molars. Based on X-ray photoelectron spectroscopy (XPS) depth profile analysis and high resolution electron microscopy of the Mg-exchanged dental enamel, a poorly ordered surface layer of approximately 10–15 nanometer thickness was identified (Figure 15). This thin layer is strongly enriched in Mg and has non-apatitic structure. Below the surface layer, the Mg content increased only moderately (up to ~3 at%) and the apatite crystal structure of enamel was preserved. As a common effect of the Mg exchanged volume, primary dental enamel exhibited about 20% increase of nanohardness, which is interpreted by strengthening of both the thin surface layer and the region below due to the decreased crystallite size and the effect of incorporated Mg, respectively [Kis et al. 2021].
Arrangement of nanocrystals was studied in the deformation zone affected by the stress field of nanoindentation imprint using transmission electron microscopy. Strong fragmentation and loss of texture was observed in this mechanically modified surface layer in both the ion exchanged and untreated dental enamel (Figure 15). Below the surface layer, textured nanostructure remained. Between the nanocrystals amorphous intercrystalline material was detected by HRTEM (Figure 16), which can serve as channel medium for the incorporating Mg ions [Kis et al. 2022 ELMINA poster].

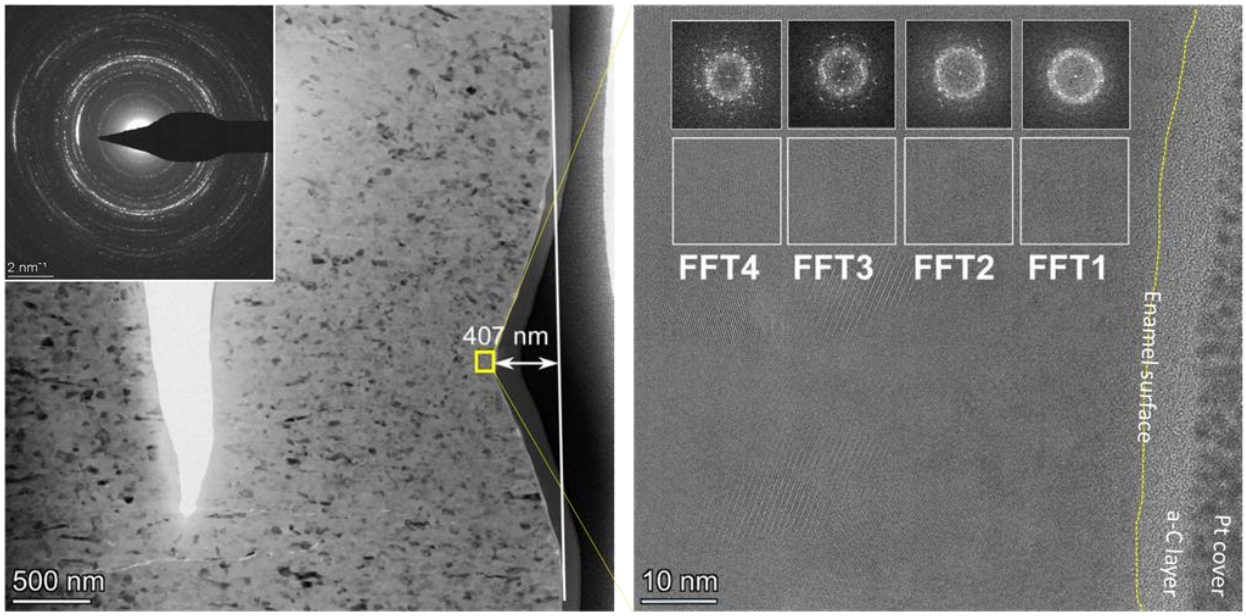

Figure 15: TEM image of cross section of the indent together with the SAED pattern. (right) HRTEM of the area indicated with yellow box on the low resolution image. FFTs made from 15x15nm areas allow to follow structural change as function of distance from enamel surface. [Kis et al. 2022 ELMINA poster]

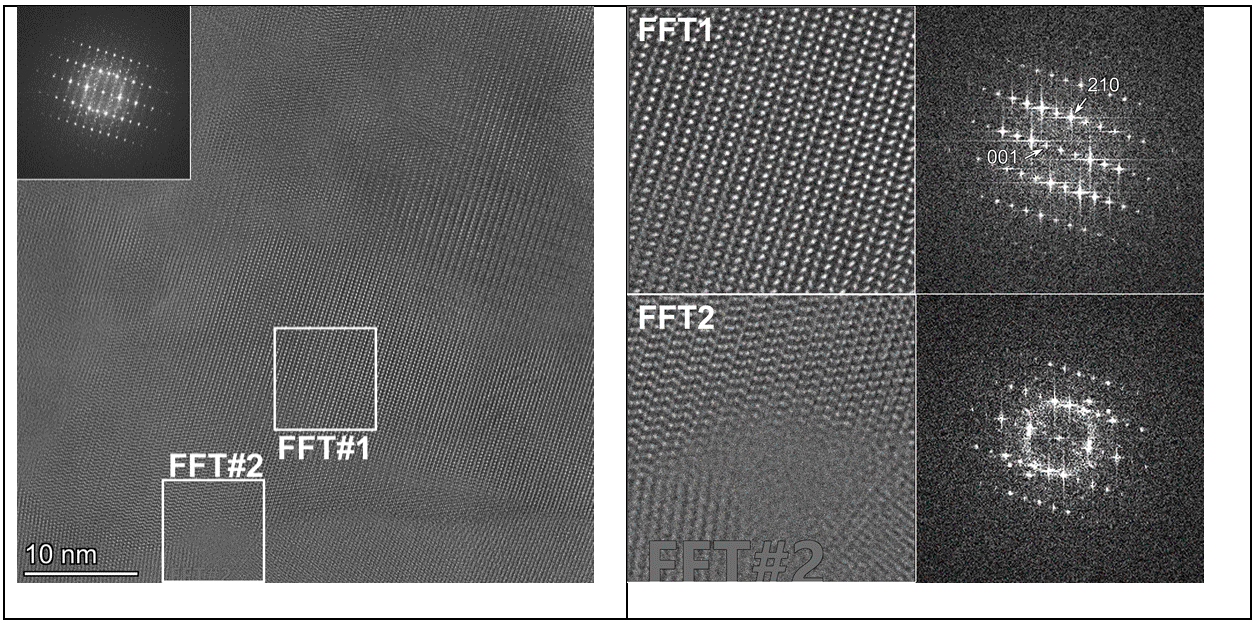

Figure 16: (left) HRTEM image at 500 µm distance from enamel surface, below the nanoindentation imprint exhibits crystalline apatite FFT. The size and orientation (crystallographic c axis of the nanocrystal is approximately perpendicular to the outer surface) indicates that at this depth the arrangement of nanocrystals is preserved. (right) Detailed FFT analysis reveals intercrystalline amorphous material. [Kis et al. 2022 ELMINA poster]

In summary, Mg exchange can induce hardness increase in dental enamel (Figure 17). This hardness increase can be attributed to (1) the fact that Mg-O bonds have more strength than Ca-O bonds and (2) a vacancy filling mechanism related to Mg incorporation, which leads to enamel apatites close to stoichiometry. Based on these experimental evidences and theoretical considerations we concluded that the observed zonation of HV in cross section of dental enamel (Figure 14) should have structural origin (Kis et al. 2021, Acta Biomater).

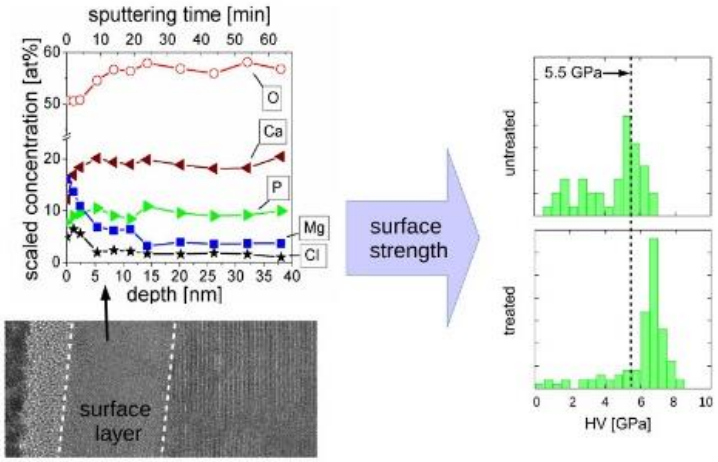

Figure 17:
(left, up) Depth distribution of enamel components (P, O, Ca, Mg and Cl) calculated from XPS analysis after removing C contamination.
(left down) HRTEM of the poorly ordered surface layer formed during Mg exchange. (right) HV distributions before and after Mg treatment. [Kis et al. 2021. Acta Biomat]

Results 3.3 Surface chemistry modifications as studied using X-ray photoelectron spectroscopy [Takács BSc thesis 2021, Sulyok et al. in preparation]

Besides mechanical performance, chemical resistance is another key property of dental enamel. Resistance to organic acids has been investigated by treating enamel samples with 0.1M citric acid solution (pH=3.45) for different timespans (120s, 1 day, 5 days) at room temperature. The dissolution was followed using XPS. To improve the reliability of quantitative XPS data, reference measurements on single crystal F-apatite of geological origin have been carried out and calibrated XPS factors were obtained.
After citric acid treatment, Ca/P ratio decreased significantly from 1.60-1.66 down to 1.54. For comparison, the same experiment was carried out on (001) crystallographic surface of single crystal F-apatite as well, which also exhibited decrease of Ca/P, however, in less extent, from 1.66 to 1.59. The decrease of Ca/P ratio of dental enamel was of the same order of magnitude for all samples, independently of the duration of soaking, which can be related to the 10 nm information depth of XPS measurement. The results indicate that citric acid solution mobilizes Ca from the apatite structure and this mobilization is faster in case of dental enamel, which is related to the nanocrystalline character [Takács BSc thesis].
An interesting byproduct of the XPS measurements was the observation that serious (up to 4 times of the nominal concentration) enrichment of fluorine occurs as function measurement time. This is supposed to be related to X-ray exposure of the samples. To fully understand the phenomenon, several X-ray irradiation experiments were carried targeting both (001) and (100) facets of single crystal F apatite samples. The fluorine development on apatite surfaces was continued until reaching a saturation and this saturated state was thoroughly investigated involving Angular Resolved XPS technics as well. According to our observations, the fluorine enrichment layer can be removed by ion sputtering and can be induced again by subsequent irradiation. The procedure was repeated several times on the same target. The excess fluorine content is limited to a relatively thin surface region (not more than a few nm), because a subsequent ion sputtering can remove it easily.
The depth distribution of fluorine species was determined using model calculations. The (001) and (100) facets exhibited different behavior. Intensive enrichment of F^{++} was going on in a narrow surface zone near the (001) face. Below a wide layer with lesser extra fluorine (F^{+}) content was measured. In case of (100) face, the high fluorine concentration F^{++} layer is absent. Though the thickness F^{+} layer seems to be different on the two faces (80 Å and 40 Å for (001) and (100) faces, respectively), practically they accumulate the same amount of fluorine. Regarding the total fluorine content, the (001) face exhibited stronger enrichment. Time development of fluorine content was also observed and registered. Under normal conditions, excess fluorine with respect to stoichiometry was detected after already 30 minutes of X-ray exposure, however a near-saturated state needed more than a day (1440 minute) of irradiation (Figure 18) at the given experimental conditions.

Based on these observations a 4-step model is proposed to explain the fluorine enrichment phenomena. (1) Mobilization: F^{-} ions are neutralized by the X-ray beam in the interaction volume. (2) Free diffusion: migration of unbounded fluorine atoms begins in random direction. As there are loose electrons (photoelectrons) in the crystal, the re-ionization is preferred. (3) Guided diffusion: surface becomes positively charged as photoelectrons escaping the sample leave positive surplus. This attracts the re-ionized F- into the very near surface zone. (4) Equilibrium: The atomic flow towards the surface results in fluorine accumulation at or nearby the surface until reaching an equilibrium concentration.

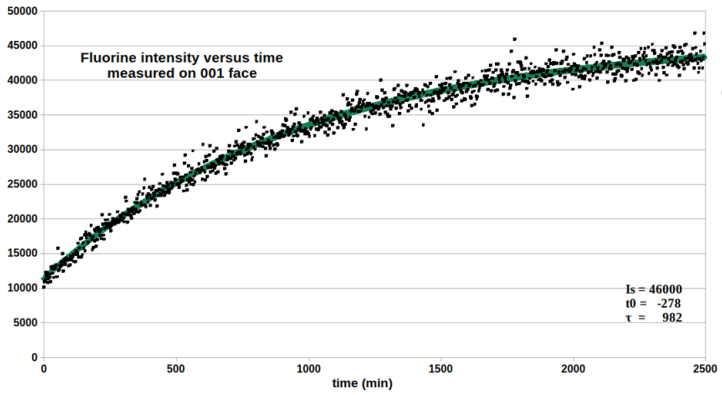

Figure 18: Fluorine intensity development on (001) face of apatite single crystal as function of irradiation time.

Results 3.4 Towards quantitative SAED of dental enamel [Kis et al. 2021 Brno Nanocon talk, Kis et al. 2022 ELMINA talk, Czigány, Kis 2022 Microscopy Research Technique paper, Kis et al. submitted, Kis et al. in preparation]

According to Results 3.2, the hardness zonation observed in cross section of primary dental enamel cannot be fully explained by changing chemical composition [Kis et al. 2021 Acta Biomater paper]. To explore the nanostructure in the highest and lowest hardness zones, pairs of FIB lamellae perpendicular to each other were taken out at 200, 600 and 1100 µm distances from the outer enamel surface for TEM investigation. As the measurement volume of the mechanical properties is on the several hundreds of nanometre scale (Figure 15), to investigate mechanical performance as function of nanostructure, such a method is needed, which provides average information of the crystal chemistry and arrangement of many-many nanocrystals, so the SAED was chosen for this purpose.

To perform high precision SAED measurements an optimized measurement and evaluation procedure was developed for our Themis Cs corrected TEM (Figure 19).

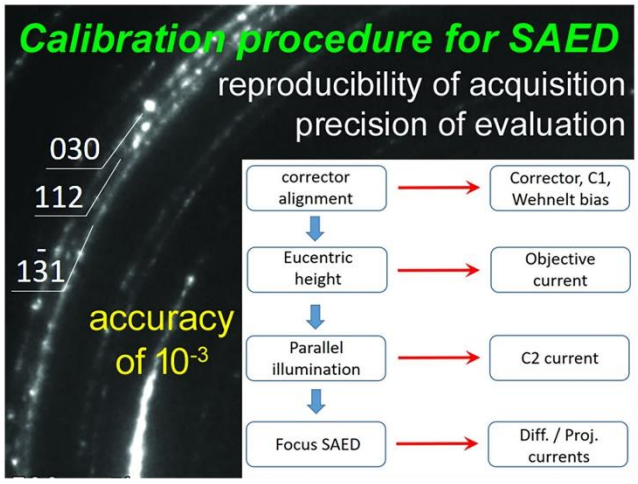

Figure 19: Proposed procedure for SAED measurements, which allows accuracy of 10^{-3}. In the background, SAED pattern of enamel apatite is shown to illustrate the benefits of the calibration procedure on the clear separation of diffraction rings spaced as closely as 0.04 Å. (1-31 and 112 rings of apatite) [Czigány, Kis 2022 MRT paper]

By careful control of specimen height and illumination conditions, it was possible to reach a session to session reproducibility of $3x10^{-4}$ for camera length in our SAED measurements. Refinements of the centre of the diffraction pattern and corrections for ellipticity of rings allowed for determining the lattice spacings with an accuracy of 10^{-3}. We analyze the effect of different error sources and reason the achieved absolute accuracy of the measurement. The achieved accuracy of 0.1% without internal standard is approaching

that of routine laboratory XRD, however, with orders of magnitude better locality. Reduction of instrumental broadening due to the elaborated evaluation procedure allows for separation of close reflections and provides more reliable ring width and thus improved input parameters for further nanostructure analysis (Czigány, Kis 2022 MRT paper).
Applying the above detailed procedure, high accuracy SAEDs were recorded from the FIB lamellae of dental enamel and for selected *hk*0 and 00*l* peaks, position and peak width were obtained, which allowed the assessment of lattice parameter ratios and crystallite size at each measured location. At all locations, the width of 002 peak was the smallest, indicating elongated crystal shape parallel to the crystallographic c axis, according to the expectations. Peak width, and thus, crystal size correlates with Mg concentration and exhibited inverse correlation with hardness (Kis et al. 2021 Brno Nanocon talk). Besides that, systematic shift of 0*kl* reflections was measured (Figure 20). These data, however, provide useful details on dental enamel nanostructure, still are insufficient for explaining the observed mechanical zonation.

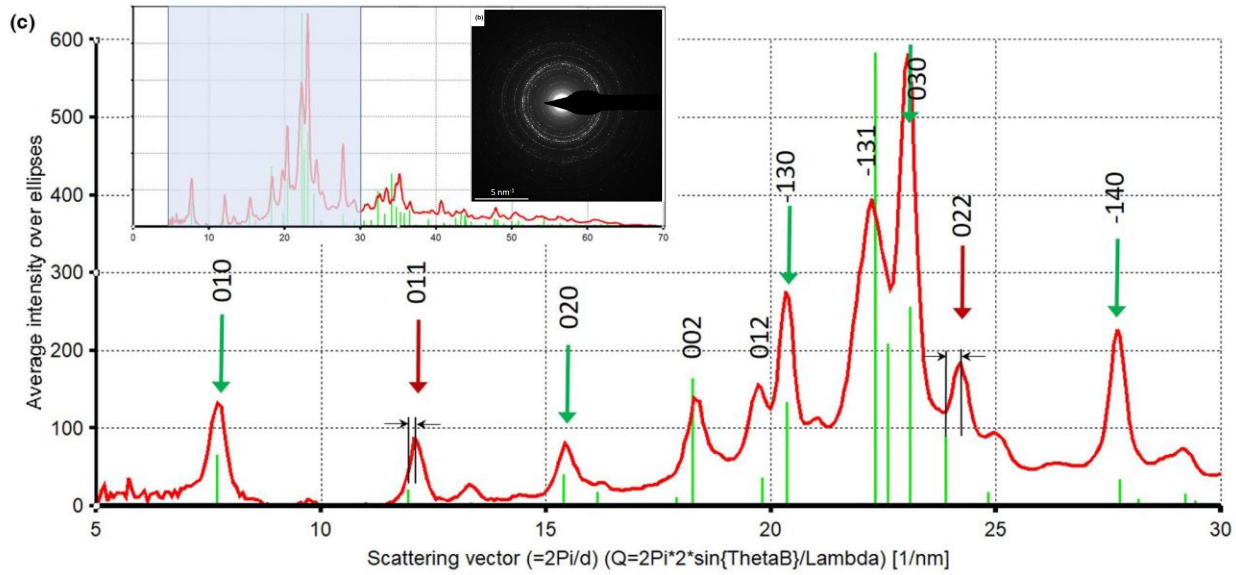

Figure 20: Integrated intensity profile of SAED pattern taken from a FIB lamella lifted out at 200 µm from outer surface. The main peaks are indexed according to hydroxylapatite structure (ICSD-26204). Green arrows indicate exact coincidence of measured *hk*0 peaks with peaks calculated from structural data. Red arrows indicate shift of 0*kl* reflections of ca 1.5% in terms of d-value with respect to hydroxyapatite structure. [Czigány, Kis 2022].

To get more detailed data on the average nanostructure, Rietveld analysis of SAED patterns was applied. Nanostructure information is included in the diffraction line profile, i.e. shape and broadening of the diffraction peaks, however, peak broadening also exhibits instrumental broadening effect, which is related to the applied experimental setup. Thus, to obtain nanostructure information from Rietveld analysis, it is of fundamental importance to separate properly the scattering angle dependent sample contribution and instrumental contribution of the TEM to peak broadening.

According to the literature (Boullay et al. *Acta Crystallogr* A70, (2014) 448–456), the determination of the instrumental broadening of a TEM requires three independent measurements and two calibration samples. As an alternative approach, we proposed a single step in-TEM procedure [Kis et al. submitted], which allows to obtain instrumental broadening function of TEM using a few layer thick graphene

calibration sample by a single SAED measurement (Figure 21). The shape of the diffraction peaks is modelled as function of scattering angle using the Caglioti relation, which can be directly applied in Rietveld analysis of electron diffraction data. During peak shape analysis, instrumental broadening parameters of the TEM are controlled separately from nanostructure related peak broadening effects contribution to a higher reliability of nanostructure information extracted from electron diffraction patterns. This procedure is based on our previous work on SAED calibration [Czigány & Kis, 2022 MRT paper] exploiting its reproducibility, the achievable ±0.1% absolute accuracy of SAED measurements and minimization of instrumental broadening. The potential of the procedure is demonstrated on hematite nanopowder and nanocrystalline thin film specimens [Kis et al. 2022 ELMINA talk].

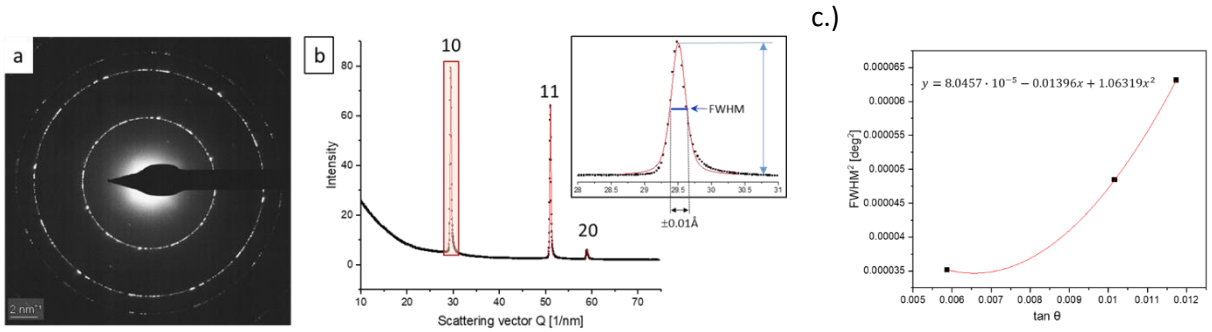

Figure 20: (a) SAED pattern taken from Pelco® graphene 3-5 support film (Ted Pella) and (b) corresponding integrated intensity profile. The 10 peak of graphene is enlarged in the insert to illustrate FWHM value characteristic of the applied measurement conditions. (c) Polynomial fit to obtain the U, V, W Caglioti parameters from the SAED pattern of P-graphene. [Kis et al. submitted]

Preliminary Rietveld analysis of SAED pattern shown on Figure 19 indicated that the peak positions marked by red arrows are not related to lattice parameter variation of hydroxylapatite, but to the presence of an additional minority phase, whitlockite, $Ca_9Mg(HPO_4)(PO_4)_6$. Depth distribution of Mg and HPO_4 measured using Raman spectrometry are in good agreement and support whitlockite formation during amelogenesis. HRTEM at 200 µm from the outer surface prove isometric non-textured whitlockite nanocrystals in between enamel apatite crystals. We suspect that the appearance of whitlockite nanocrystals, by breaking the gradual anisotropy of the enamel structure, has measurable effect of mechanical performance. The conditions of whitlockite formation in relation with enamel apatite crystallization will be investigated in the future. Actually undergraduate student Mr. András Szabó (Eötvös University) investigates whitlockites of inorganic and organic origin.

Publications

Papers:

[1] Kis V.K., Czigány Z., Dallos Z., Nagy D., Dódony I.: ***HRTEM study of individual bone apatite nanocrystals reveals symmetry reduction with respect to P63/m apatite***, MATERIALS SCIENCE & ENGINEERING C-MATERIALS FOR BIOLOGICAL APPLICATIONS 104: 109966, 2019 IF: 6.259

[2] Dallos Zsolt, Kis Viktória Kovács, Kristály Ferenc, Dódony István: ***Leaching mechanism of bioapatite in carbonate-saturated water***, CRYSTENGCOMM 22: (16) pp. 2788-2794., 2020 IF: 3.545

[3] M. Fábián 1,2, * , Zs. Kovács 3 , J. L. Lábár 1 I. Székács 1 , and V. Kovács Kis 1,4, *: ***Network structure and thermal properties of bioactive (SiO 2 –CaO–Na 2 O–P 2 O 5) glasses***, J. Mater. Sci. February 2020, Volume 55, Issue 6, pp 2303–2320, 2020. IF: 4.22

[4] Kis VK., Sulyok A, Hegedűs M, Kovács I, Rózsa N, Kovács Zs: ***Magnesium incorporation into primary dental enamel and its effect on mechanical properties***, Acta Biomaterialia, Volume 120, 15 January 2021, Pages 104-115, 2021 IF: 8.94

[5] Kovács Zs, Fábián M, Szász N, Székács I, Kis-Kovacs V: ***Tracking the initial stage of bioactive layer formation on Si-Ca-Na-P oxide glasses by nanoindentation***, JOURNAL OF NON-CRYSTALLINE SOLIDS 581: 121416, 2022 IF: 4.12

[6] Czigány Zsolt, Kis Viktória Kovács: ***Acquisition and evaluation procedure to improve the accuracy of SAED***, MICROSCOPY RESEARCH AND TECHNIQUE in press, 2022 IF:2.769

[7] Máté Hegedűs, Viktória K. Kis, Ábel Szabó, Ivett Kovács, Noémi Rózsa, Zsolt Kovács: ***Enamel prism and crystallite orientation dependence of mechanical properties of primary dental enamel*** submitted to Acta Biomat.

[8] Viktória Kovács Kis, Zsolt Kovács, Zsolt Czigány: ***Single step in-TEM determination of electron diffraction peak shape and its application in Rietveld analysis of nanocrystalline materials***. Submitted to Microscopy and Microanalysis

Papers in preparation:

[1] Sulyok, A, Takács, D, Kis, V.K.: ***X-ray induced fluorine segregation on apatite minerals***

[2] Hegedűs, M., Kis, V.K., Szabó, Á., Kovács, Zs: ***Quantitative evaluation of enamel prism arrangement based on image processing technique***

[3] Kis, V.K., Hegedűs, M., Czigány, Zs., Aradi, L.E., Radnóczi, Gy.Z., Rózsa, N, Kovács, Zs.: ***Whitlockite appears in the hardest zone of dental enamel***

Conference talks and poster presentations:

[1] V.K. Kis, M. Fábián and J. Lábár: ***Mineralogical applications of ePDF analysis of amorphous materials - need for validation***, Mini-Workshop on ePDF analysis, 28-29 March, 2018, Ulm, Germany. invited talk, 2018

[2] Kovács Kis, Viktória and Fábián, Margit and Székács, Inna and Kovács, Ivett and Lábár, János and Kovács, Zsolt: ***Structural investigations on bioactive glasses***, Magyar Mikroszkópos Konferencia, Siófok Hungary. talk, 2018

[3] Dallos, Zsolt, Kovács Kis, Viktória, Kristály, Ferenc and Dódony, István: ***Heating experiments on bone apatite to observe structural alterations.***, n: International Microscopy Conference, Sydney, Australia. Poster presentation, 2018

[4] Krisztián Kiss, Tamás Szeniczey, Kinga Karlinger, Zsuzsanna Mészáros Kis, Enikő Szvák, Erika Molnár, Antónia Marcsik, Antal Sklánitz, Lénárd Szabó, Zsolt Dallos, Viktória Kovács Kis, Krisztina Buczkó, Tamás Hajdu: ***A possible case of metastatic cancer from Kehida-Fövenyes (7th-8th century A.D.)***, In: Novak, Mario; Cvitkušić, Barbara; Janković, Ivor; Jarec, Morana; Missoni, Saša (szerk.) 22nd European Meeting of the Paleopathology Association. Book of Abstracts, Institute for Anthropological Research (2018) pp. 35-35., 2018 *

[5] V. Kovács Kis, Zs. Czigány, M. Hegedűs, Zs. Kovács: ***Texture properties of primary dental enamel along prism growth direction.***, Abstract Book, 13th International Conference on Nanomaterials, Oct 20-22, 2021, Brno, Czech Republic, 2021

[6] Zs. Czigány, V. Kovács Kis: ***Standardization and evaluation of electron diffraction measurements for characterization of bioapatite in human dental enamel***, Abstract Book, 13th International Conference on Nanomaterials, Oct 20-22, 2021, Brno, Czech Republic, 2021

[7] Kovácsné Kis Viktória, Czigány Zsolt, Kovács Zsolt: ***Nanokristályos anyagok Rietveld analízise elektrondiffrakciós mérések alapján***, In: Kittel, Ágnes; Solymosi, Katalin; Barna, László (szerk.) A Magyar Mikroszkópos Társaság 2022 Konferenciájának Kivonatkönyve, Magyar Mikroszkópos Társaság (2022) pp. 126-129., 2022

[8] Máté Hegedűs, László Előd Aradi, Viktória Kovácsné Kis, Zsolt Kovács: ***Anizotrópia vizsgálata fogzománcban pásztázó elektronmikroszkópos és Raman spektroszkópos módszerekkel***, In: Kittel, Ágnes; Solymosi, Katalin; Barna, László (szerk.) A Magyar Mikroszkópos Társaság 2022 Konferenciájának Kivonatkönyve, Magyar Mikroszkópos Társaság (2022) pp. 44-47., 2022

[9] Máté Hegedűs, Zsolt Kovács, László Előd Aradi, Viktória Kovács Kis, Noémi Rózsa: ***Structural anisotropy in primary dental enamel and its relation to mechanical properties***, Szegedi Fogorvosnapok, 2022 *

[10] Viktória K. Kis, Attila Sulyok, Máté Hegedűs, Noémi Rózsa, Zsolt Kovács: ***TEM Study on the Nanostructure Change of Primary Dental Enamel Subjected to Mechanical and Chemical Surface Modifications***, In: Velimir, R. Radmilović; Vuk, V. Radmilović (szerk.) Second InternatIonal conference on electron microscopy of nanostructures, Serbian Academy of Sciences and Arts (2022) pp. 154-155., 2022 *

[11] Viktoria Kovács Kis, Zsolt Czigány, Zsolt Kovács: ***Microstructure Investigation of Nanocrystalline Materials Using Electron Diffraction Based Rietveld Analysis – Approximation of Instrumental Broadening***, In: Velimir, R. Radmilović; Vuk, V. Radmilović (szerk.) Second InternatIonal conference on electron microscopy of nanostructures, Serbian Academy of Sciences and Arts (2022) pp. 98-99., 2022 *

Diploma thesis:

[1] Hegedűs Máté (témavezetők: Kis Viktória, Kovács Zsolt): ***Humán tejfog zománcon és különböző kalcium-foszfátokon végzett ioncserés vizsgálatok***, ELTE BSc Thesis, 2019

[2] Hegedűs Máté (témavezetők: Kis Viktória, Kovács Zsolt): ***Mechanical characterization of human primary enamel***, ELTE MSc Thesis, 2021

[3] Takács Dániel (témavezető Sulyok Attila): ***Emberi tejfog fogzománcának vizsgálata XPS módszerrel***, Óbuda University, BSc Thesis, 2021